IOSR Journal of Applied Physics (IOSR-JAP)
e-ISSN: 2278-4861.Volume 17, Issue 4 Ser. 1 (Jul. – Aug. 2025), PP 94-102
www.iosrjournals.org

Optimization Of Iron Oxide Nanoparticle Biosynthesis Using Response Surface Method

Vipin Kumar* & Ajay Kumar**
**Professor, Deptt of Physics, SKD University, Hanumangarh*
***Research Scholar at Deptt of Physics, SKD University, Hanumangarh*
*** Asst. Prof., Department of Physics, Dr. B.A Govt. College Sriganganagar*
Corresponding author: ajayghoran92@gmail.com

Abstract: *Iron oxide nanoparticles were synthesized through a green synthesis method with Dalbergia sissoo leaf extract being used as a reducing/stabilizing agent. The method presented an eco-friendly, straightforward way to synthesize iron oxide nanoparticles. We explored the influence of key factors in the synthesis, including precursor concentration of 0.1 – 1.0 mM, pH (6 to 9), reaction time (12 to 48 hours), and temperature (25 - 60 °C). We noted the production of a black color during the emergence of the nanoparticles throughout the reaction. This confirmed that iron oxide nanoparticles had formed. UV-Vis spectroscopy indicated that we had created iron oxide nanoparticles. There was a considerable absorbance in the range of 200-400 nm. Studies have reported trends of a strong absorbance between this range for iron oxide nanoparticles. We determined the optical band gap between the synthesized iron oxide nanoparticles and obtained band gap values which ranged from 2.56 to 3.05 eV. These values fall within an acceptable range of reported properties of iron oxide nanoparticles. Our results confirmed the formation of iron oxide nanoparticles and alignment with expected behaviors. Box–Behnken Design (BBD) was utilized to optimize the conditions for the synthesis of iron oxide nanoparticles. Since the factors were studied at three levels, 27 experiments were carried out. Data from the experiments was analyzed using Analysis of Variance (ANOVA) and Response Surface Methodology (RSM). The predictive ability of the model was high. The R^2 value was 95.18%. The Adjusted R^2 value was 89.56%. ANOVA identified the precursor concentration, pH and temperature as significant factors. Each of these factors profoundly impacted the yield of nanoparticles. The most predicted yield was 97.70%, which was predicted at conditions of 1.0mM precursor concentration, pH 9, and temperature of 25 °C for 25.46 hours. The Dalbergia sissoo extract was used to synthesis the nanoparticles, which is a green and eco-friendly approach to synthesis. It allows for nanoparticle characteristics to be controlled. It has potential for sustainable nanoparticle production.*
Keywords*: Box–Behnken Design,* Dalbergia sissoo*, green synthesis, Iron oxide nanoparticles, Response Surface Methodology, UV–Vis spectroscopy,*

Highlights

- Iron oxide nanoparticles were synthesized through a green synthesis method using leaf extract of Dalbergia sissoo.
- Absorbance readings in the UV spectra (200–400 nm) demonstrated that Dalbergia sissoo leaves produced iron oxide nanoparticles.
- The optical band gap analysis showed values between (2.56 -3.05 eV), consistent with other literature (Safitri et al., 2021; Soltanpour et al., 2024).
- Response Surface methodology (RSM) and Box–Behnken Design was used to optimize the synthesis process.
- The maximum yield of 97.70% predicted yield of iron oxide nanoparticles was obtained from the optimised conditions.

I. Introduction

Nanoparticles are very tiny particles that are between 1 and 100 nanometers in size. Nanoparticles also have some interesting features. They have a relatively high surface area. They can also change some of their optical and electrical properties which can be advantageous in a variety of applications, including drug delivery, biosensing, pollution remediation, and dsys Macromolecular Science which are often oriented to new biomaterials (Khan et al., 2019).

In medicine, nanoparticles can enhance the efficacy of drugs. They can solubilize drugs and enhance stability, but more importantly, they are capable of delivering drugs to a precise location using targeted drug delivery behaviours which can result in fewer side effects and thus, better therapeutic outcomes (Khan et al., 2019).

One environmentally friendly approach for making nanoparticles is through green synthesis. Green synthesis uses plants or microbes to synthesize nanoparticles and it usually does not require hazardous chemicals or excessive energy (Iravani, 2011). In biology, green synthesis is often associated with producing safe and biocompatible nanoparticles (Bhattacharya & Mukherjee, 2008).

Iron is the most abundant material on earth, physically and chemically. Iron is found in earth's rocks as minerals like magnetite and hematite. Humans have been using iron from ancient times. Volcanic eruptions and meteorites are believed to have helped release large amounts of iron, and iron occurs in the Earth's crust as well as its core ("The Iron Age of Civilization," n.d.). Iron is a part of everyday life as it includes its use as a resource in biological organisms. For example, Iron is an integral part of hemoglobin (an oxygen carrier) in animals, and it plays a role in carbon metabolism and chlorophyll metabolism in plants (Blaszczak-Boxe, 2017).

When iron is prepared in nanoparticle form, it properties change significantly. Bulk iron is a metallic element, however, at the nanoscale, iron can behave as a semiconductor and demonstrate strong ferromagnetic to ferrimagnetic properties. For example, when iron is reduced to the nanoscale, the iron can show significant magnetic properties, such as superparamagnetism and having a low value for coercivity (which can help with false positive diagnostic imaging using MRI, targeted drug methodology, or cancer thermal therapy) ("Iron Nanoparticles: Properties and Applications," n.d.).

Iron oxide forms such as Fe_3O_4, γ-Fe_2O_3, and α-Fe_2O_3 have growing usage in the electronics, medical, and catalyst industries, successfully demonstrated the ability to decompose dye and metal and even successfully combine with nanocomposites for photocatalytic degradation; iron oxide -containing materials include the characteristics to absorb both UV and visible light thus have a wide range of progressive solar energy systems. However, they are not performant in those systems as they have a disadvantage of clustering into assemblies in soluble forms and reactivity with other metals which can result in oxidation.

These particles can act as catalysts for making fuels and to support a range of reactions in environmental applications such as Fischer–Tropsch synthesis (Huber, 2005). New approaches here too have evaluated iron oxide nanoparticles are produced in different ways... They can be physically produced, chemically produced, or made through green synthesis (Iqbal et al., 2017).

In this research study, green synthesis was conducted. The experimental nutrient rich plant materials were kept of Sebastopol Rigor (Gareav), using to produced iron oxide nanoparticles. The plant used in this study is Dalbergia sissoo Roxb, which includes the common name Indian Rosewood. This plant is indigenous to a large area in India and is used in Ayurveda and Unani medecine, specifically for health contributing benefit of alleviating pain, fever, and herbs against bacterial infection (Bhattacharya et al., 2014). The leaves of the plant were used to extract to nanoparticles of iron oxide where the leaves were used to reduce and stabilize the iron ions.

To optimize the nanoparticles in this study we used response surface methodology (RSM) to assess multiple levels of factors, and optimize these factors to find the best contributions (Kumari & Gupta, 2019). During this process we decided to use a Box–Behnken design that assessed 27 combinations and validated the experimental number of 18 with experience and analysis of the factors (iron salt, pH, time of reaction and incubation of temperature). The experimental data was analyzed using ANOVA and regression approaches. The processing of results was achieved using Minitab® software (v15.1.30.0) (Watson et al., 2016; Ye et al., 2017).

II. Materials and Method

2.1 Materials and Preparation of Plant Leaf Extract

Analytical grade ferrous sulfate heptahydrate ($FeSO_4 \cdot 7H_2O$) was used as the source of iron (Fe) for the synthesis of the biogenic iron oxide nanoparticles (FeONPs). Double-distilled water was used for all experiments. Whatman No. 1 filter paper and borosilicate glass beakers (80 mL and 250 mL) were used as part of the synthesis. A set of 27 borosil test tubes (15 mL each) and laboratory-grade 95% ethanol were also obtained. Sodium hydroxide (NaOH) pellets were purchased locally.

The equipment that was used included a REMI magnetic stirrer with hot plate (Model 2MLH). A LABTRONICS digital pH meter (Model LT-11) was used to monitor pH. In addition, a digital weighing balance and laboratory thermometer were used for precise measurement. Samples were preserved in a fridge. Spectral measurements were made using JASCO UV–Vis spectrophotometer (Model V-750).

Fresh Dalbergia sissoo (Shisham) leaves were procured from the botanical garden of Dr. Bhimrao Ambedkar Government College in Sri Ganganagar, Rajasthan, and were washed with tap water to remove dirt, soap, and residue, and washed again under distilled water (Siddique et al., 2024).

Ten grams of cleaned leaves were air dried in ambient air. The leaves were chopped to small pieces. The chopped leaves were then mixed with 100 mL distilled water in a 250 mL borosilicate beaker. This mixture was then separately heated until it reached 80 °C (approx.) which was maintained for 45 minutes.

The extract was filtered using two methods. The first method was using muslin cloth. The second method using Whatman No. 1 filter paper (Khan et al., 2020). A reddish liquid extract was collected and preserved in a sterile glass bottle at 4 °C until required (Singh et al., 2012).

2.2 Methodology: Experimentation Design

To optimize the synthesis of nanoparticles, we applied Response Surface Methodology (RSM). More specifically, we selected a Box–Behnken Design (BBD) which allows us to evaluate linear, interaction, and quadratic processes. This design tested multiple process variables and combinations of variables.

Table 1: Included factors and their ranges:

Sr. No.	Factor name	Factor maximum value	Factor minimum value	Middle value
1.	precursor concentration	1 mM	0.1 mM	0.55 mM
2.	Temperature	25 ˚C	60 ˚C	42.5 ˚C
3.	pH	6	9	7.5
4.	reaction timing	12 hours	48 hours	30 hours

This statistical design, also minimizes the number of experimental runs, which makes best use of our time and resources, without sacrificing accuracy. Ultimately, our goal was to find the optimal synthesis parameters of fabrication conditions that would yield maximum nanoparticles.

Table 2: Coded Levels of Synthesis Parameters

Factor	Actual value	Level coded
Precursor Concentration	0.1 M	-1
	0.55 mM	0
	1mM	1
Temperature	25˚C	-1
	42.5 ˚C	0
	60 ˚C	1
pH	6	-1
	7.5	0
	9	1
Time	12 h	-1
	30 h	0
	48 h	1

Ferrous sulphate heptahydrate ($FeSO_4 \cdot 7H_2O$) was used as an iron source. In distilled water, three concentrations; 0.1 mM, 0.55 mM, and 1.0 mM, were prepared and each reaction was done in a separate test tube. The ratio of plant extract to metal salt solution was held constant at 1:4.

The pH was adjusted carefully between 6 and 9, which was done by adding 0.1 N sodium hydroxide solution drop by drop. The reaction tubes were allowed to stand undisturbed and were incubated for 12, 30, or 48 h, per plan.

During the reaction there was a visible change in colour, from reddish-brown to black, indicating the proposed formation of iron oxide nanoparticles and black precipitate settled at the bottom of the tubes.

After the synthesis, all samples were diluted tenfold and analysis was performed using UV–Visible spectroscopy. Analysis was performed using a JASCO V-750 UV/Vis spectrophotometer and absorbance readings were a good way of monitoring nanoparticle formation.

The area under each absorbance curve could therefore be calculated and could then be used to determine the optimum conditions that provide the higher yield, i.e., maximum nanoparticle production (Kamath et al., 2020; Liaqat et al., 2022; Kartini et al., 2020).

III. Result and Discussion

3.1 UV–Vis Spectrum Analysis

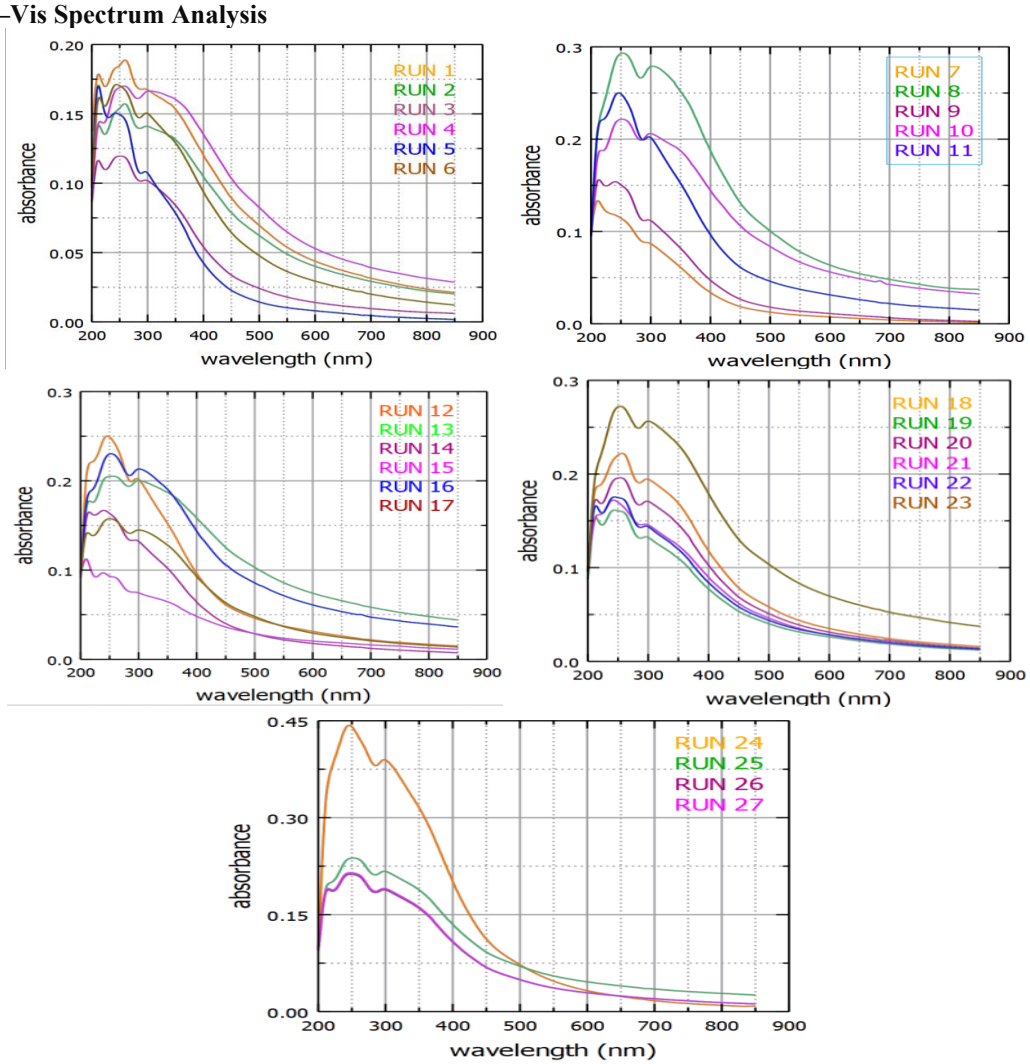

Figure 1: Obtained graphs from sets of experiment for optimization procedure

Table 3: sets of experiments and corresponding yield

Run Order	Concentration (mM)	Time (Hour)	pH	Temperature (°C)	Yield
1	0.10	12	7.5	42.5	25.527
2	1.00	12	7.5	42.5	52.240
3	0.10	48	7.5	42.5	15.250
4	1.00	48	7.5	42.5	57.996
5	0.10	30	6.0	42.5	26.102
6	1.00	30	6.0	42.5	43.435
7	0.10	30	9.0	42.5	34.036
8	1.00	30	9.0	42.5	88.250
9	0.10	30	7.5	25.0	27.610
10	1.00	30	7.5	25.0	66.279
11	0.10	30	7.5	60.0	50.324
12	1.00	30	7.5	60.0	72.882
13	0.55	12	6.0	42.5	34.976

14	0.55	48	6.0	42.5	68.736
15	0.55	12	9.0	42.5	25.375
16	0.55	48	9.0	42.5	68.786
17	0.55	12	7.5	25.0	42.324
18	0.55	48	7.5	25.0	54.492
19	0.55	12	7.5	60.0	41.855
20	0.55	48	7.5	60.0	48.177
21	0.55	30	6.0	25.0	43.025
22	0.55	30	9.0	25.0	41.855
23	0.55	30	6.0	60.0	81.117
24	0.55	30	9.0	60.0	51.665
25	0.55	30	7.5	42.5	63.250
26	0.55	30	7.5	42.5	56.450
27	0.55	30	7.5	42.5	57.450

The UV–Visible spectrum for the synthesized iron oxide nanoparticles is shown in Figure 1. Significant UV absorbance was seen in the UV range starting from 200 nm to 400 nm. A noticeable peak is identified in between 250 nm to 300 nm. This is a common Surface Plasmon Resonance (SPR) behavior of iron nanoparticles.

Previous research validates this result. Karpagavinayagam and Vedhi (2018) reported SPR peaks from 295 nm to 301 nm. Hussain et al. (2023) reported peaks from between 230 nm and 290 nm. Saranya et al. (2017) also reported values in the 250–350 nm range. Ashrafi-Saiedlou et al. (2025) demonstrated iron oxide nanoparticles have significant UV–Vis absorption across wavelengths. Dadashi et al. (2015) showed absorbance peaks can range from 190 nm to 900 nm depending on particle formation and their properties.

In general, these UV absorbance characteristics are expected from the internal electronic configuration of the nanoparticles. The SPR behavior is govern by the optical constants of the nanoparticle and its surrounding, and Mie theory explains the shifts in the curve due to particle size, shape and surface properties.

Iron oxide nanoparticles will generally behave as direct band gap semiconductors. In this study, the band gap ranged from 2.56 eV to 3.05 eV, in previous studies. Safitri et al. (2021) and Soltanpour et al. (2024) previously reported similar values. This band gap is useful for photocatalysis and optoelectronics.

On the basis of these graphs yield was obtained by calculating absorbance curve area. (Chowdhury et al., 2016)

3.2 Statistics Validation by ANOVA

Table 4: Outcomes of Analysis of Variance (ANOVA)

Source	DF	Seq SS	Adj SS	Adj MS	F	P
Regression	14	8956.79	8956.79	639.77	18.22	0.000
Linear	4	6351.92	6351.92	1587.98	45.22	0.000
Square	4	2029.77	2029.77	507.44	14.45	0.000
Interaction	6	575.10	575.10	95.85	2.73	0.066
Lack-of-Fit	10	395.16	395.16	39.52	3.01	0.275
Pure Error	2	26.27	26.27	13.13	-	-
Total	26	9378.22	-	-	-	-

Statistical validation of the model in predicting the response was completed using ANOVA, and the p-value < 0.001, therefore the model is considered highly significant. The F-value was 18.22, which supports the level of significance (Table 4).

The total sum of squares in the dataset was 9378.22, and the model explained a total of 8956.79 units. Therefore, the model is capable of capturing most of the variation in the data set.

The linear terms had the greatest effect. The F-value was 45.22, with a p-value < 0.001, suggesting some form of strong linear relationship between the input variables and the response.

The quadratic terms did have a significant effect. The F-value was 14.45, $p < 0.001$. This again supports the argument the response curve was not flat, and maybe slightly curvilinear, so there are linear and non-linear trends in the dataset.

The interaction terms were close to significant at F-value 2.73, and p-value 0.066. Their potential significance suggests there may be some interaction effect present, though is likely not very substantial.

Lack-of-fit tests were also performed to assess the fit of the model. The lack of fit F-value was 3.01, p-value = 0.275. Because this value exceeds 0.05, the model adequately fits the data. There is no significant lack of fit.

This statistical analysis has validated that the factors assessed in this study significantly influenced the response. The model can be considered statistically valid and useful for prediction purposes.

3.3 Model Summary and Regression Equation

A regression analysis was performed to determine the effect of four different variables on synthesis response in order to model such variability to as accurately as possible predict yield of iron oxide nanoparticles. The model contained linear, interaction, and quadratic terms.

From the Table 5, it is possible to see that the linear terms were significant. The linear terms included precursor concentration (A), reaction time (B), and pH (C). Every linear term had a p-value of less than 0.05. This implies that these factors had a strong influence on yield of iron oxide nanoparticles. Temperature (D) was only marginally significant while having a p-value of slightly less than 0.05; this still implies a valuable albeit weaker influence on yield.

Table 5: Model summary

Term	Coefficient	SE Coefficient	T-Value	P-Value
Constant	59.0657	3.421	17.263	<0.001
A	16.8437	1.711	9.846	<0.001
B	-4.6011	1.711	-2.690	0.020
C	14.6052	1.711	8.537	<0.001
D	3.3368	1.711	1.951	0.075
A^2	-8.8357	2.566	-3.443	0.005
B^2	-14.6811	2.566	-5.721	<0.001
C^2	-0.7909	2.566	-0.308	0.763
D^2	4.7922	2.566	1.868	0.086
A×B	4.0370	2.963	1.362	0.198
A×C	9.2202	2.963	3.112	0.009
A×D	-4.0352	2.963	-1.362	0.198
B×C	-4.2027	2.963	-1.418	0.182
B×D	2.6775	2.963	0.904	0.384
C×D	-1.1612	2.963	-0.392	0.702

S (Standard Error of Regression)	6.08144
PRESS (Prediction Residual Error Sum of Squares)	2502.08
R^2 (Coefficient of Determination)	95.18 %
Adjusted R^2	89.56 %
Predicted R^2	72.83 %

Of the interaction terms, only the two factor interactions of precursor concentration and pH (A × C) was statistically significant with a p-value of 0.009. This exhibits a synergy behavior between the two factors which both contributed to the particle yield.

The quadratic terms A^2 and B^2, also show significance with p-values being less than 0.05 and indicate that curvature on the response surface does exist and should be utilized for optimum production.

There was satisfactory predictive strength showed by the model. The coefficient of determination (R^2) for the model was 0.9518; the adjusted R^2 is 0.895. These values imply that the model explains the majority of variance, while limiting unreliability.

The overall F-value for the model was 18.22. The associated p-value was 0.00 implying that the model is both statistically significant, and valid.

A second-order polynomial regression equation was developed for the model based on coded variables where each factor (A, B, C, D) was normalized within its range. The model contains all significant terms linear, quadratic and interaction components.

The regression model can now be used to predict yield of nanoparticles for a variety of synthesis conditions, as well as to determine the best factors for optimization of desired results.

$Y= 59.0657+16.8437A - 4.6011B + 14.6052C + 3.3368D - 8.8357A^2 - 14.6811B^2 - 0.7909C^2 + 4.7922D^2 + 4.0370AB + 9.2202AC - 4.0352AD - 4.2027BC + 2.6775BD - 1.1612CD$

3.4 Optimization and Model Validation

Response surface and contour plots were used to study the effects of the variables. The response surface and contour plots clearly illustrated how the process variables affected yield. Strong interaction effects were observed. It was observed with highest incidence with precursor concentration(A) vs reaction time(B), and that concentration(A) vs pH(C) also showed strong interactions.

The response surface revealed noticeable curvature. This confirmed that the system behaved in a non-linear manner and that yield was not heavily influenced in isolation from the other factors. However, there were possibly combinations that were indicative of the yield value.

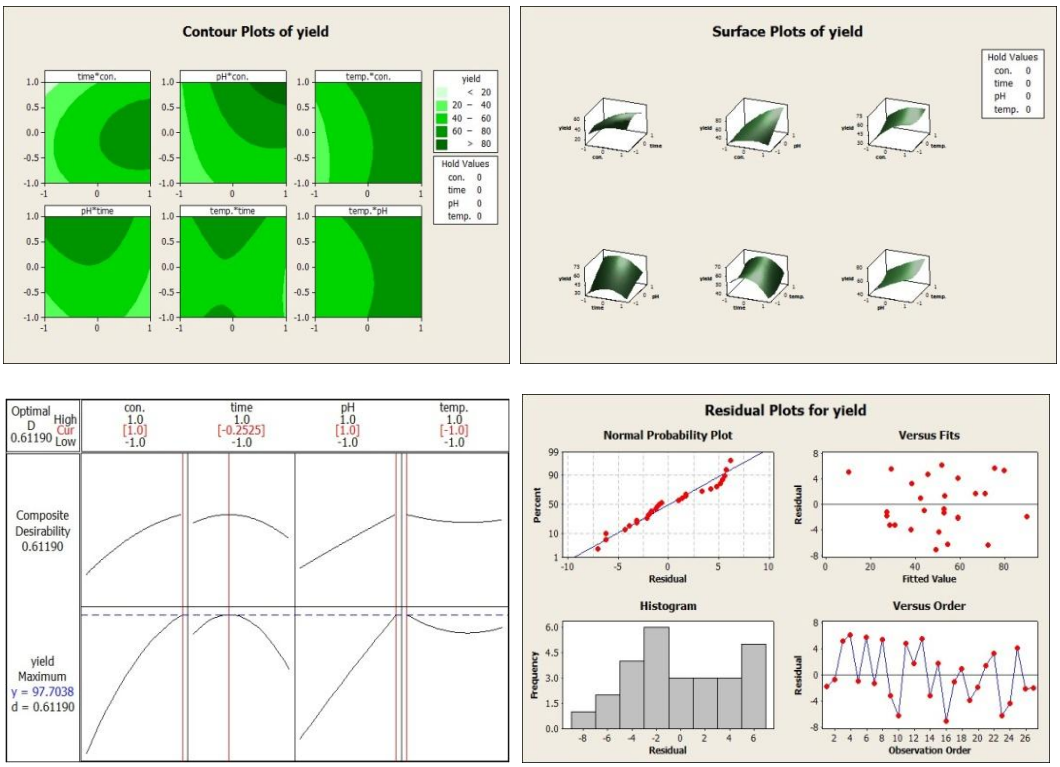

Figure 2: RSM plots

Optimization was performed using the desirability function method. The highest predicted yield was 97.70 which was achieved at the following coded conditions: A=1.0, B=–0.2525, C= 1.0, and D=–1.0. The composite desirability value for this point was 0.6119 which represents a fair tradeoff across all variables.

Model validation was conducted using residual analysis. The normal probability plot of residuals fit a nearly straight line. This confirms that the assumption of normality was met. The residual versus fitted values plot displayed sufficiently random scatter suggesting constant variance, or homoscedasticity.

There was no discernible trend present for the residuals versus order plot indicating no sequential bias was present in the data. The histogram of the residuals depicted a symmetric distribution centered at the zero value. All diagnostic plots support the accuracy of the model.

Overall, the data indicates that yield can be optimized by working to the right concentrations of time, pH, and temperature. An accurate model now exists to further synthesize the same nanoparticles in the future.

Iron oxide nanoparticles from all trials were confirmed to be direct band gap semiconductors. The band gap values were determined to range from 2.56 eV to 3.05 eV. Together, with previous work, these values are consistent across the previous literature (Safitri et al., 2021; Soltanpour et al., 2024).

IV. Conclusion

Iron oxide nanoparticles were prepared successfully. The procedure followed was a green route for preparation. The reduction and stabilizing agent was the Dalbergia sissoo leaf extract. The color change observed in the solution indicated that the nanoparticles formed. This change occurred when the color of the solution changed to black that inferred nanoparticle formation occurred.

The UV-Visible spectroscopy also indicated a very precise absorbance was produced; the absorbance was seen in the spectrum between the range of 200 and 400 nm. The optical band gap was calculated to be between

2.56 to 3.05 eV values which is in agreement with studies done previously on semiconducting iron oxide nanoparticles (Safitri et al., 2021; Soltanpour et al., 2024).

The synthesis process optimization was performed again in this study using Response Surface Methodology (RSM) techniques. The study used a Box-Behnken Design technique and created a quadratic regression model with R^2 of 95.18% and adjusted R^2 of 89.5% that described the variability of the dataset well.

Using surface and contour plots to visualize the key factors reported, precursor concentration, pH, and temperature were the three factors that had the largest effect on yield of nanoparticles, or were considered sensitive.

The quadratic regression model predicts that the best yield will happen at specific conditions, which were 1.0 mmol of precursor concentration, the reaction time was determined to be 25.46 hours, the pH for the reaction to take place was determined to be a pH of 9, and the temperature of the reaction needed to occur at 25 °C. The predicted maximum theoretical yield was cited as 97.7%.

In summary, these findings show that it is feasible to utilize Dalbergia sissoo extract as an effective and secure green, plant-based way of synthesizing iron nanoparticles and that it is constructive and within the context of sustainable yield for any system to facilitate controlling the yield of the experiment through understanding and utilizing the experimental variables as a statistical process, approach.

V. Future Scope

- However, this method of biological fabrication can be extrapolated to prepare other metal nanoparticles from a different variety of medicinal plants.
- More sophisticated spectral techniques, including FTIR, XRD, and TEM, can be used to validate the structure of the nanoparticles.
- Iron oxide nanoparticles can also be explored for antibacterial, antifungal or photocatalytic properties.
- The physical properties can also be explored for use in solar energy harvesting and water purification systems.
- The model can be further applied and optimized using hybrid optimization approaches such as the GA-RSM or the ANN-RSM.
- There can be plans for utilizing scale-up studies for the sake of developing an approach fit for industrial-level production of nanoparticles.
- If Dalbergia sissoo is to be utilized, too, there is an argument for local sustainability of the process, making it a reasonably economical endeavor, as well.
- As additional work is pursued through a comparative study with chemical and microbial synthesis approaches, hopefully more benefits can be apparent.
- Further work can also be undertaken to explore the potential of nanoparticle morphology effects on performance in biomedical applications.
- These points strengthen the future applicability of development in sustainable, eco-friendly nanomaterials with tunable properties.

References

[1]. Ali, A., Zafar, H., Zia, M., Haq, I. U., Phull, A. R., Ali, J. S., & Hussain, A. (2016). Synthesis, characterization, applications, and challenges of iron oxide nanoparticles. *Nanotechnology, Science and Applications, 9*, 49–67. https://doi.org/10.2147/nsa.s99986

[2]. Ashrafi-Saiedlou, S., Rasouli-Sadaghiani, M., Fattahi, M., & Ghosta, Y. (2025). Biosynthesis and characterization of iron oxide nanoparticles fabricated using cell-free supernatant of *Pseudomonas fluorescens* for antibacterial, antifungal, antioxidant, and photocatalytic applications. *Scientific Reports, 15*(1). https://doi.org/10.1038/s41598-024-84974-0

[3]. Bhattacharya, M., Singh, A., & Ramrakhyani, C. (2014). *Dalbergia sissoo* – An important medical plant. *Journal of Medicinal Plants Studies, 2*(2), 76–82. http://www.plantsjournal.com

[4]. Bhattacharya, R., & Mukherjee, P. (2008). Biological properties of "naked" metal nanoparticles. *Advanced Drug Delivery Reviews, 60*(11), 1289–1306. https://doi.org/10.1016/j.addr.2008.03.013

[5]. Blaszczak-Boxe, A. (2017). Facts about iron. *Live Science*. https://www.livescience.com/29263-iron.html

[6]. Chowdhury, S., Yusof, F., Faruck, M. O., & Sulaiman, N. (2016). Process optimization of silver nanoparticle synthesis using response surface methodology. *Procedia Engineering, 148*, 992–999. https://doi.org/10.1016/j.proeng.2016.06.552

[7]. Dadashi, S., Poursalehi, R., & Delavari, H. (2015). Structural and optical properties of pure iron and iron oxide nanoparticles prepared via pulsed Nd:YAG laser ablation in liquid. *Procedia Materials Science, 11*, 722–726. https://doi.org/10.1016/j.mspro.2015.11.052

[8]. Huber, D. L. (2005). Synthesis, properties, and applications of iron nanoparticles. *Small, 1*(5), 482–501. https://doi.org/10.1002/smll.200500006

[9]. Hussain, A., Yasar, M., Ahmad, G., Ijaz, M., Aziz, A., Nawaz, M. G., ... Faisal, S. (2023, August 1). Synthesis, characterization, and applications of iron oxide nanoparticles. *National Library of Medicine (PMC)*. https://pmc.ncbi.nlm.nih.gov/articles/PMC10321464/

[10]. Iqbal, A., Iqbal, K., Li, B., Gong, D., & Qin, W. (2017). Recent advances in iron nanoparticles: Preparation, properties, biological and environmental application. *Journal of Nanoscience and Nanotechnology, 17*(7), 4386–4409. https://doi.org/10.1166/jnn.2017.14196

[11]. Iravani, S. (2011). Green synthesis of metal nanoparticles using plants. *Green Chemistry, 13*(10), 2638–2650. https://doi.org/10.1039/c1gc15386b

[12]. Kamath, V., Chandra, P., & Jeppu, G. P. (2020). Comparative study of using five different leaf extracts in the green synthesis of iron oxide nanoparticles for removal of arsenic from water. *International Journal of Phytoremediation, 22*(12), 1278–1294. https://doi.org/10.1080/15226514.2020.1765139

[13]. Karpagavinayagam, P., & Vedhi, C. (2018). Green synthesis of iron oxide nanoparticles using *Avicennia marina* flower extract. *Vacuum, 160*, 286–292. https://doi.org/10.1016/j.vacuum.2018.11.043

[14]. Kartini, K., Alviani, A., Anjarwati, D., Fanany, A. F., Sukweenadhi, J., & Avanti, C. (2020). Process optimization for green synthesis of silver nanoparticles using Indonesian medicinal plant extracts. *Processes, 8*(8), 998. https://doi.org/10.3390/pr8080998

[15]. Khan, I., Saeed, K., & Khan, I. (2017). Nanoparticles: Properties, applications and toxicities. *Arabian Journal of Chemistry, 12*(7), 908–931. https://doi.org/10.1016/j.arabjc.2017.05.011

[16]. Khan, M. I., Akhtar, M. N., Ashraf, N., Najeeb, J., Munir, H., Awan, T. I., ... Kabli, M. R. (2020). Green synthesis of magnesium oxide nanoparticles using *Dalbergia sissoo* extract for photocatalytic activity and antibacterial efficacy. *Applied Nanoscience, 10*(7), 2351–2364. https://doi.org/10.1007/s13204-020-01414-x

[17]. Kumari, M., & Gupta, S. K. (2019). Response surface methodological (RSM) approach for optimizing the removal of trihalomethanes (THMs) and its precursor's by surfactant modified magnetic nanoadsorbents (sMNP) – An endeavor to diminish probable cancer risk. *Scientific Reports, 9*(1). https://doi.org/10.1038/s41598-019-54902-8

[18]. Liaqat, N., Jahan, N., Khalil-Ur-Rahman, N., Anwar, T., & Qureshi, H. (2022). Green synthesized silver nanoparticles: Optimization, characterization, antimicrobial activity, and cytotoxicity study by hemolysis assay. *Frontiers in Chemistry, 10*. https://doi.org/10.3389/fchem.2022.952006

[19]. Quintero-Quiroz, C., Acevedo, N., Zapata-Giraldo, J., Botero, L. E., Quintero, J., Zárate-Triviño, D., ... Pérez, V. Z. (2019). Optimization of silver nanoparticle synthesis by chemical reduction and evaluation of its antimicrobial and toxic activity. *Biomaterials Research, 23*(1). https://doi.org/10.1186/s40824-019-0173-y

[20]. Safitri, I., Wibowo, Y. G., Rosarina, D., & Sudibyo, N. (2021). Synthesis and characterization of magnetite (Fe_3O_4) nanoparticles from iron sand in Batanghari Beach. *IOP Conference Series: Materials Science and Engineering, 1011*(1), 012020. https://doi.org/10.1088/1757-899X/1011/1/012020

[21]. Saranya, S., Vijayarani, K., & Pavithra, S. (2017). Green synthesis of iron nanoparticles using aqueous extract of *Musa ornata* flower sheath against pathogenic bacteria. *Indian Journal of Pharmaceutical Sciences, 79*(5). https://doi.org/10.4172/pharmaceutical-sciences.1000280

[22]. Siddique, M. H., Sadia, M., Muzammil, S., Saqalein, M., Ashraf, A., Hayat, S., ... Abd-Allah, E. F. (2024). Biofabrication of copper oxide nanoparticles using *Dalbergia sisso* leaf extract for antibacterial, antibiofilm and antioxidant activities. *Scientific Reports, 14*(1). https://doi.org/10.1038/s41598-024-83199-5

[23]. Singh, C., Baboota, R. K., Naik, P. K., & Singh, H. (2012). Biocompatible synthesis of silver and gold nanoparticles using leaf extract of *Dalbergia sissoo*. *Advanced Materials Letters, 3*(4), 279–285. https://doi.org/10.5185/amlett.2011.10312

[24]. Soltanpour, P., Naderali, R., & Mabhouti, K. (2024). Comparative study on structural, morphological, and optical properties of MS/Fe_3O_4 nanocomposites and M-doped Fe_3O_4 nanopowders (M = Mn, Zn). *Scientific Reports, 14*(1). https://doi.org/10.1038/s41598-024-72026-6

[25]. Tauc, J., Grigorovici, R., & Vancu, A. (1966). Optical properties and electronic structure of amorphous germanium. *Physica Status Solidi (b), 15*(2), 627–637. https://doi.org/10.1002/pssb.19660150224

[26]. The iron age of civilization. (n.d.). *POSCO Newsroom*. https://newsroom.posco.com/en/the-iron-age-of-civilization/

[27]. Watson, M. A., Tubić, A., Agbaba, J., Nikić, J., Maletić, S., Jazić, J. M., & Dalmacija, B. (2016). Response surface methodology investigation into the interactions between arsenic and humic acid in water during the coagulation process. *Journal of Hazardous Materials, 312*, 150–158. https://doi.org/10.1016/j.jhazmat.2016.03.002

[28]. Ye, G., Ma, L., Li, L., Liu, J., Yuan, S., & Huang, G. (2017). Application of Box–Behnken design and response surface methodology for modeling and optimization of batch flotation of coal. *International Journal of Coal Preparation and Utilization, 40*(2), 131–145. https://doi.org/10.1080/19392699.2017.1350657